

Evolution of magnetism in Pd-substituted Ce_2RhIn_8 single crystals

M. Kratochvilova¹, K. Uhlirva¹, J. Prokleska¹, S. Danis¹, P. Cermak¹, V. Sechovsky¹

¹ *Department of Condensed Matter Physics, Charles University in Prague, Faculty of Mathematics and Physics, Ke Karlovu 5, 121 16 Prague 2, Czech Republic*

Keywords: antiferromagnetism, T - x phase diagram, specific heat, Ce_2RhIn_8

Abstract:

The evolution of magnetism and superconductivity in $\text{Ce}_2\text{Rh}_{1-x}\text{Pd}_x\text{In}_8$ solid solutions has been studied within the entire concentration range by means of thermodynamic and magnetic measurements at ambient pressure and at temperatures between 0.35 K and room temperature. For this purpose, single crystals with Pd concentrations $x = 0, 0.10, 0.15, 0.30, 0.45, 0.55, 0.85$ and 1 have been grown from In self-flux and characterized by x-ray diffraction and microprobe analysis. Starting from the antiferromagnet Ce_2RhIn_8 , the Néel temperature gradually decreases with increasing Pd concentration and the antiferromagnetism has disappeared for $x \geq 0.45$. Superconductivity has been observed only for Ce_2PdIn_8 .

1. Introduction

$\text{Ce}_n\text{TIn}_{3n+2}$ ($n = 1, 2$; $T = \text{Co, Ir, Rh}$) heavy-fermion (HF) compounds have been attracting attention of scientific community for almost two decades owing to coexistence of magnetic order and superconductivity in a wide area of the temperature-pressure-composition phase diagrams [1]. In the vicinity of the magnetic quantum critical point (QCP), unconventional superconductivity has been reported [2]. The compounds crystallize in the tetragonal $\text{Ho}_n\text{CoGa}_{3n+2}$ -type of structure (P4/mmm). The layered character of the structure is determined by various sequences of TIn_2 and CeIn_3 basic building blocks stacked along the c -axis. The dimensionality of the structure, which spans from 3D (CeIn_3) to quasi-2D (CeTIn_5) seems to control the type of ground state. The desire to examine this aspect in more detail has motivated further efforts to synthesize and investigate new members of the $\text{Ce}_n\text{TIn}_{3n+2}$ family [3].

Ce_2RhIn_8 is a prototype example of a $\text{Ce}_n\text{TIn}_{3n+2}$ HF antiferromagnet exhibiting pressure induced superconductivity [2]. It orders below $T_N = 2.8$ K in a commensurate antiferromagnetic (AF) structure with $(\frac{1}{2}, \frac{1}{2}, 0)$ propagation vector and with the Ce magnetic moments making an angle of 52° with the basal plane and successively displays a second transition to the ground-state incommensurate magnetic structure at $T_{LN} = 1.65$ K [4,5]. Analysis of thermal-expansion, magnetovolume and specific-heat data indicates that the physical properties of Ce_2RhIn_8 result from competition between magnetic exchange, Kondo and crystal-field interactions⁵. Upon increasing the magnetic field along the a -axis, T_N of Ce_2RhIn_8 increases and two magnetic-field-induced transitions appear. The phase transitions divide the phase diagram into several regions with different magnetic structures which have not been studied microscopically so far. T_N decreases monotonically with increasing magnetic field applied along the c -axis. The ground state of Ce_2RhIn_8 can be tuned from AF to a superconducting (SC) not only by applying pressure [6] but also by substitutions [7,8]. Hydrostatic pressure induces a SC phase which coexists with the AF phase up to a pressure of 1.7 GPa and, at higher pressures, only the superconductivity remains [6]. Compared to its

more-2D analogue, the CeRhIn₅ system, the effect of various substitutions in Ce₂RhIn₈ has been studied only poorly. Particularly interesting is the evolution of the critical temperatures in the case of transition-metal-site substitutions. Ir-rich samples of the Ce₂Rh_{1-x}Ir_xIn₈ series undergo a SC transition; another SC state in the low-Ir-concentration region can be induced by applying hydrostatic pressure [7]. The effect of Ir substitution exhibits similarities with the behavior of CeRh_{1-x}Ir_xIn₅ [9]. Co substitution for Rh suppresses the magnetism monotonically with no signs of superconductivity up to $x = 0.6$ [10]. The non-isoelectronic Cd substitution [8] at the In site enhances the AF interactions in Ce₂RhIn₈. A recent ARPES study [11] on a Ce₂RhIn_{7.79}Cd_{0.21} sample has revealed suppression of the hybridization gap by Cd substitution. On the other hand, adding one extra electron by substitution of non-isoelectronic Sn suppresses the magnetism gradually [12]. Studies of substitutions for Ce have been focused on La [13] and Pr [14] as substituents. Both types of substitutions suppress the magnetic-ordering temperature due to the dilution effect.

In contrast to Ce₂RhIn₈, Ce₂PdIn₈ is an ambient-pressure HF superconductor with a sample dependent SC transition temperature with the highest value of $T_c \sim 0.7$ K [15-17]. No indications of magnetic ordering have been found. The compound has been linked to CeCoIn₅ because of its ambient-pressure superconductivity and non-Fermi-liquid behavior [18]. Because the growth of pure Ce₂PdIn₈ single crystals has turned out to be very difficult, only a very limited number of measurements performed on pure single crystalline samples have been reported [3,15] and no attempt of tuning of the quantum criticality by substitution has been made. According to a recent study [19] of the related CeRh_{1-x}Pd_xIn₅ system, the AF state of CeRh_{1-x}Pd_xIn₅ is almost independent of the Pd content (up to $x = 0.25$) while the pressure-induced superconductivity is enhanced. The results suggest that at higher Pd concentration the ground state of CeRhIn₅ might turn into a SC state already at ambient pressure. The aim of the present work is to study the evolution of antiferromagnetism and superconductivity in Ce₂Rh_{1-x}Pd_xIn₈ compounds with varying composition of the 4*d*-transition-metal sublattice. We report on results of single-crystal growth of selected Rh-Pd concentrations, characterization of the chemical composition and crystal structure, measurements of the temperature dependence of the specific heat in various magnetic fields and magnetization measurements as a function of temperature and magnetic field.

2. Sample synthesis and characterization

The Ce₂Rh_{1-x}Pd_xIn₈ single crystals have been grown from In self-flux by a technology procedure analogous to the one used for Ce₂PdIn₈ [3,15] and CeRh_{1-x}Pd_xIn₅ [19]. The growth composition Ce:Rh_{1-y}Pd_y:In = 2:1:30 was chosen for samples with lower Pd content $y \leq 0.5$; for the samples with $y \geq 0.5$, the stoichiometry 1:3:45-55 was used as it improved the homogeneity and avoided the growth of undesired phases such as CeIn₃ similarly to the growth procedure of Ce₂PdIn₈ described in literature [15]. The batches were heated up to 950 °C, kept at this temperature for 10 hours to let the mixture homogenize properly and then cooled down slowly (~ 3 °C/h) to 500 °C, where the remaining flux was decanted.

The samples were checked carefully by microprobe analysis using a Scanning Electron Microscope (SEM) Tescan Mira LMH equipped with an energy dispersive x-ray detector (EDX) Bruker AXS and ESPRIT software. The issue regarding the determination of the real Rh-Pd contents by microprobe analysis has been thoroughly discussed in the case of CeRh_{1-x}Pd_xIn₅ samples [19]. Representative crystals with final concentrations $x = 0, 0.1, 0.15, 0.28, 0.45, 0.55, 0.85$ and 1 have been selected. No crystals with Pd

concentration between 0.55 and 0.85 have been found in any growth batch. In this concentration region, we have not succeeded in preparing homogeneous single crystals free of spurious phases. Similar to $\text{CeRh}_{1-x}\text{Pd}_x\text{In}_5$ crystals [19], the actual Pd content in the samples has been found to be lower than the nominal Pd concentration of the melt. Within the crystals selected for bulk measurements, deviations from the composition $\Delta x = 0.02\text{-}0.05$ have been observed. For crystals with $0.3 < x < 1$ the deviation was somewhat larger being $\Delta x = 0.11$. The single crystals had a plate-like shape with the c -axis perpendicular to the largest surface. The mass of the samples selected for measurements varied from 0.3 to 4 mg.

The lattice parameters have been determined by single-crystal x-ray diffraction using Rigaku RAPID II. To confirm the crystal orientation, the Laue method was used. The specific heat was measured in the temperature range 0.35-300 K using PPMS 9T (*Quantum Design*) equipped with a Helium-3 option for low-temperature operation. The magnetization was measured in the temperature range 1.8-300 K using a MPMS 7 T.

3. Results and discussion

Single-crystal x-ray diffraction confirmed that the $\text{Ce}_2\text{Rh}_{1-x}\text{Pd}_x\text{In}_8$ crystals adopt the Ho_2CoGa_8 -structure type for all prepared concentrations $x = 0.10, 0.15, 0.30, 0.45, 0.55$ and 0.85 . With increasing x , the room-temperature lattice parameter a increases slightly while c decreases (see Fig. 1). As a result, the unit-cell volume increases with increasing Pd content whereas the c/a ratio decreases by about 1 %. The change of the c/a ratio is similar to corresponding changes in Ir- (0.9 %) and Co-substituted (0.6 %) samples [7,10] in the whole concentration range.

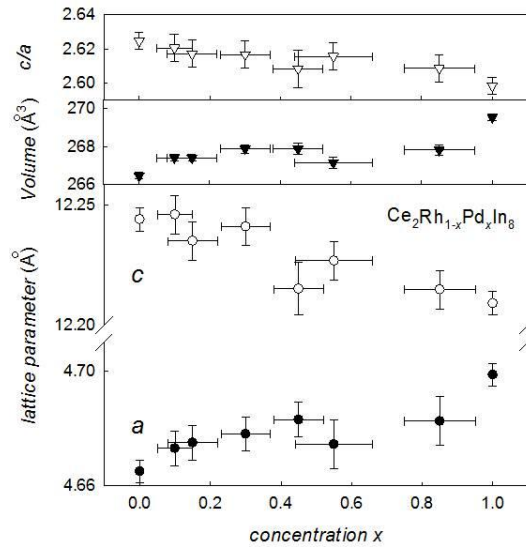


Fig. 1. Lattice parameters a and c , c/a ratio and unit-cell volume of $\text{Ce}_2\text{Rh}_{1-x}\text{Pd}_x\text{In}_8$ compounds. The data for Ce_2PdIn_8 have been taken from literature [15].

In Fig. 2, the specific heat of $\text{Ce}_2\text{Rh}_{1-x}\text{Pd}_x\text{In}_8$ for various Pd concentrations is shown in the C_p/T vs. T representation. For $x = 0$, the pronounced peak at $T_N = 2.85$ K reflects the well-known transition of Ce_2RhIn_8 to commensurate AF ordering [2]. At lower temperatures, additional anomaly at $T_{LN} = 1.45$ K is observed which can be ascribed to a transition from the commensurate magnetic order existing between T_{LN} and T_N , to the ground-state incommensurate order reported in literature [4]. This order-to-order transition is absent in

samples with $x \geq 0.1$. The Néel temperature gradually decreases with increasing Pd concentration. For the $x = 0.45$ sample, no magnetic phase transition is observed at temperatures accessible with our experimental setup (≥ 0.35 K). As T_N is suppressed, a pronounced upturn of the C/T curve appears at low temperatures for the $x = 0.55$ sample which might be a sign of critical quantum AF fluctuations [20] (see inset in Fig. 2). For the $x = 0.85$ sample, the low-temperature upturn is already hardly visible and it is completely suppressed for Ce_2PdIn_8 . In the Ce_2PdIn_8 crystal, superconductivity is observed below $T_c = 0.55$ K, in agreement with literature results discussed in Ref. 15. The value of T_c of Ce_2PdIn_8 samples may vary between 0.5 and 0.7 K, but none of the $\text{Ce}_2\text{Rh}_{1-x}\text{Pd}_x\text{In}_8$ crystals, which contain Rh, shows any sign of a transition to the SC state at temperatures down to 0.35 K.

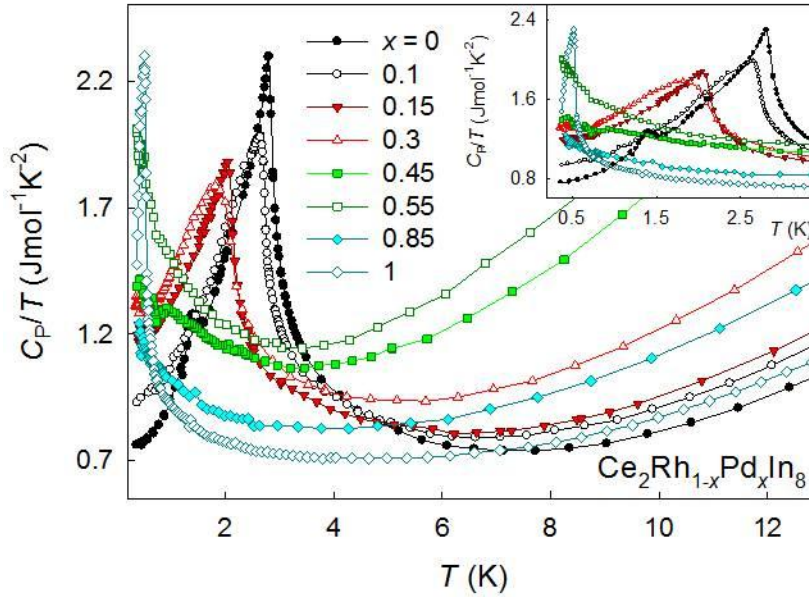


Fig. 2. Temperature dependence of the specific heat (plotted as C_p/T vs T) of the $\text{Ce}_2\text{Rh}_{1-x}\text{Pd}_x\text{In}_8$ compounds for various Pd concentrations in zero magnetic field. The inset depicts the low-temperature region.

The values of the Sommerfeld coefficient γ , which have been determined from linear fits of $C/T = \gamma + \beta T^2$ dependences in the interval $8 \text{ K} < T < 13 \text{ K}$, are shown in the phase diagram in Fig. 5. The value of γ monotonously increases with increasing Pd content from $240 \text{ mJ mol}^{-1}(\text{Ce})\text{K}^{-2}$ for Ce_2RhIn_8 up to the maximum value of $490 \text{ mJ mol}^{-1}(\text{Ce})\text{K}^{-2}$ for $\text{Ce}_2\text{Rh}_{0.45}\text{Pd}_{0.55}\text{In}_8$, which is close to the critical Pd concentration for antiferromagnetism (the evolution of T_N and γ with increasing x is shown in Fig. 5). For the sample with $x = 0.85$, γ is dramatically reduced and it further decreases for Ce_2PdIn_8 , exhibiting a value comparable with the γ value for Ce_2RhIn_8 . To allow an estimate of the magnetic entropy, the phonon term βT^2 was subtracted from the C/T data. At T_N , a $4f$ contribution of about $0.38 R \ln 2$ to the entropy S_{4f} of Ce_2RhIn_8 has been determined and, for $\text{Ce}_2\text{Rh}_{0.7}\text{Pd}_{0.3}\text{In}_8$, a contribution of about $0.24 R \ln 2$. Kondo screening of the ordered Ce moments [21] probably causes that only a small fraction of the magnetic entropy is released. The influence of the Pd content on the Kondo temperature T_K within the substitution series has been analyzed in more detail. There are several methods of estimating the Kondo temperature and they may lead to different values of T_K . However, usually a satisfactory agreement is achieved in general trends of the T_K evolution within the series [4,22]. Being aware of these constraints in the present study,

the value of T_K was derived from the specific heat and from magnetic-susceptibility data. Using specific-heat data, the evaluation of T_K was interpreted in terms of a simple two-level model considering the reduction of magnetic entropy at T_N . This approach considers the expression

$$\frac{\Delta S}{R} = \ln\left(1 + \exp\left(\frac{-T_K}{T_C}\right)\right) + \frac{T_K}{T_C} \left(\frac{\exp(-T_K/T_C)}{1 + \exp(-T_K/T_C)}\right) \quad (1)$$

which has been applied to the ferromagnetic $\text{CeNi}_x\text{Pt}_{1-x}$ series in the work of Blanco *et al.* [22]. For Ce_2RhIn_8 , we have obtained $T_K \approx 6$ K which is of the same order of magnitude as $T_K \approx 10$ K reported by Malinowski *et al.* [4]. Further increase of the Kondo temperature of $T_K \approx 7.5$ K for the Pd concentration $x = 0.15$ and $T_K \approx 12$ K for $x = 0.30$ was observed simultaneously with an increase of the coefficient γ and a decrease of the Néel temperature.

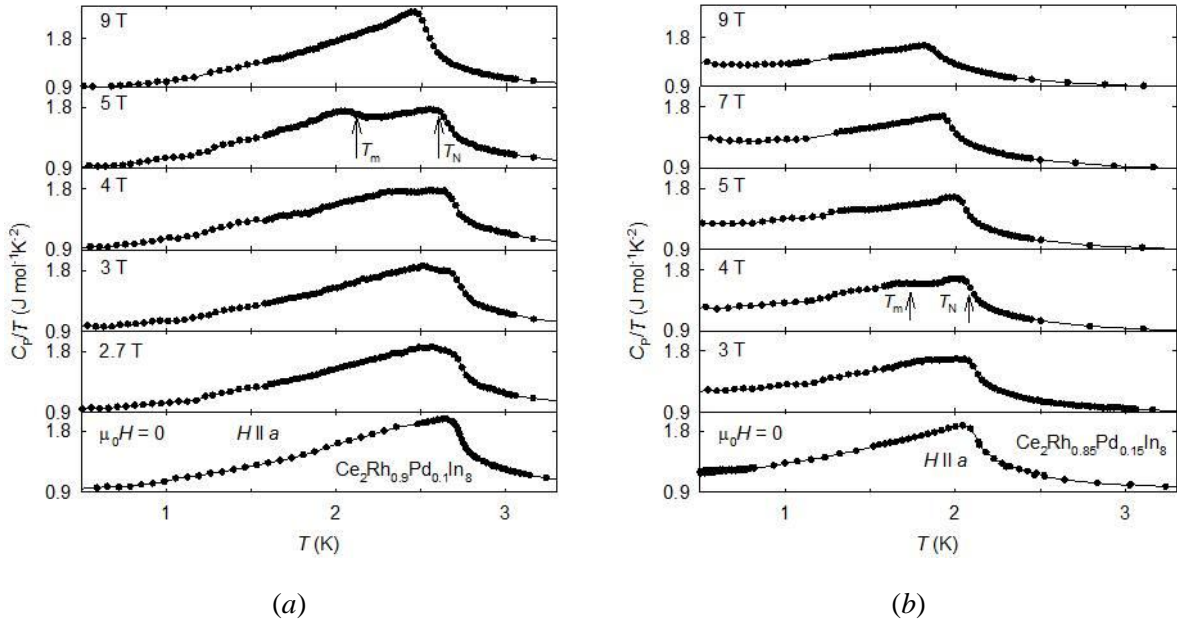


Fig. 3. Low-temperature part of the specific heat of (a) $\text{Ce}_2\text{Rh}_{0.9}\text{Pd}_{0.1}\text{In}_8$ and (b) $\text{Ce}_2\text{Rh}_{0.85}\text{Pd}_{0.15}\text{In}_8$, measured at various magnetic fields applied along the a -axis. The arrows indicate the transition temperatures T_N and T_m .

The temperature dependence of the specific heat of $\text{Ce}_2\text{Rh}_{1-x}\text{Pd}_x\text{In}_8$ compounds with $x = 0.1, 0.15$ in various magnetic fields is shown in Fig. 3. As the evolution of magnetism is only modest for the magnetic field applied along the c -axis [23], we studied the effect of magnetic field applied within the basal plane, along the a -axis. A magnetic field-induced transition shows up at $T_m \approx 2.3$ K ($T_m \approx 1.7$ K) in $\text{Ce}_2\text{Rh}_{0.9}\text{Pd}_{0.1}\text{In}_8$ ($\text{Ce}_2\text{Rh}_{0.85}\text{Pd}_{0.15}\text{In}_8$) in a field of about 4 T and moves to lower temperatures when the field is increased. For samples with $x > 0.15$ (not shown), the magnetic field-induced transitions are completely suppressed and only the AF transition remains. Both transition temperatures T_m and T_N shift to lower temperatures with increasing Pd concentration, similar to the $\text{CeRh}_{1-x}\text{Pd}_x\text{In}_5$ system [19]. The sensitivity of T_m to the Pd concentration is stronger in the $\text{Ce}_2\text{Rh}_{1-x}\text{Pd}_x\text{In}_8$ system in line with the behavior of T_N . The magnetic-field-induced transitions at T_1 and T_2 observed in Ce_2RhIn_8 [23] are smeared out in the Pd-substituted samples. Thus, the magnetic phase below T_m cannot be identified directly with one of the induced phases in the T - H phase diagram (same notation as

in Ref. 23 is used). One can speculate that the phase II is suppressed by the increasing Pd substitution; however, no microscopic study of magnetic structure was performed to support this scenario.

In order to study the magnetocrystalline anisotropy and the Kondo screening, the magnetic susceptibility $M(T)/H$ of $\text{Ce}_2\text{Rh}_{1-x}\text{Pd}_x\text{In}_8$ ($x = 0, 0.15, 0.85, 1$) was measured up to room temperature in magnetic fields applied along both the principal crystallographic directions. One can immediately recognize similarities between the low-temperature behavior of the magnetic susceptibility of Ce_2PdIn_8 and $\text{Ce}_2\text{Rh}_{0.15}\text{Pd}_{0.85}\text{In}_8$, while the susceptibility of $\text{Ce}_2\text{Rh}_{0.85}\text{Pd}_{0.15}\text{In}_8$ resembles more the behavior of Ce_2RhIn_8 , as expected (see Fig. 4). At temperatures above 50 K (100 K), the a -axis (c -axis) reciprocal susceptibility obeys the Curie-Weiss law (see inset of Fig. 4); the linear fit provides the values for the paramagnetic Curie temperature θ_p and the effective magnetic moment μ_{eff} listed in Table 1. The magnetic moments μ_{eff} of the substituted samples are somewhat smaller than the Hund's rule value of $2.54 \mu_B$ for a free Ce^{3+} ion. Together with the pronounced deviation of $1/\chi(T)$ from linear behavior at lower temperatures, this can be ascribed to an interplay of Kondo and crystal-field interactions, similar to the crystal-field effects reported for CeRhIn_5 [24] and $\text{CeRh}_{1-x}\text{Pd}_x\text{In}_5$ [19].

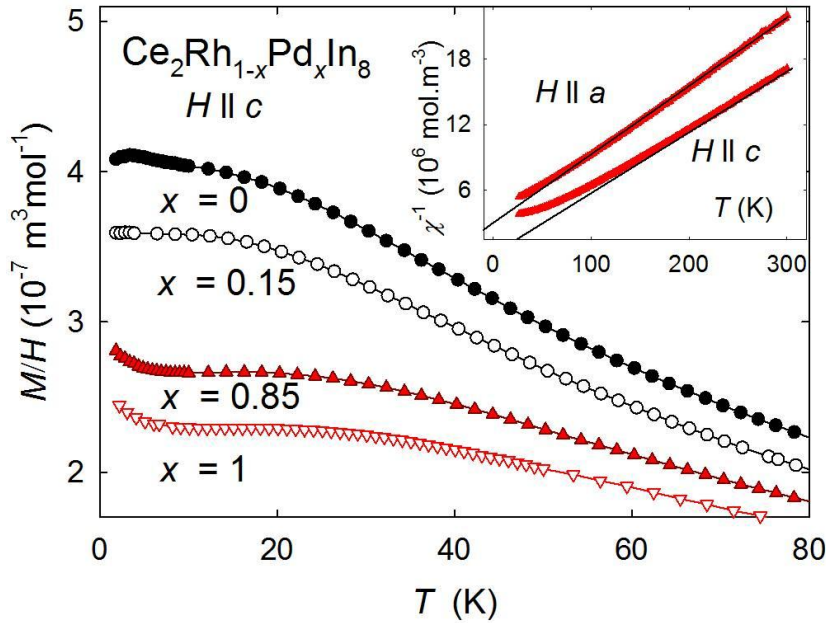


Fig. 4. Temperature dependence of the magnetic susceptibility M/H of $\text{Ce}_2\text{Rh}_{1-x}\text{Pd}_x\text{In}_8$ ($x = 0, 0.15, 0.85, 1$) measured in a magnetic field of 5 T applied along the c -axis. The inset shows the reciprocal magnetic susceptibility of $\text{Ce}_2\text{Rh}_{0.15}\text{Pd}_{0.85}\text{In}_8$ in the whole temperature range up to 300 K in magnetic fields applied along the a - and c -axis. The lines represent the fits to the Curie-Weiss law.

According to Hewson [25], the order of magnitude of the Kondo temperature T_K can be estimated from the paramagnetic Curie temperature using the formula $|\theta_p|/4$. One can immediately see a significant difference of the θ_p value for Ce_2PdIn_8 and the substituted samples likely reflecting the unique SC ground state of Ce_2PdIn_8 within the series. Considering the concentration evolution of θ_p^a , T_K decreases first from $T_K = 17$ K for Ce_2RhIn_8 to 12 K for $\text{Ce}_2\text{Rh}_{0.15}\text{Pd}_{0.85}\text{In}_8$ and it increases again for Ce_2PdIn_8 ($T_K = 23$ K). The concentration evolution of θ_p^c is non-monotonous with a weak tendency to increase from

$T_K \sim 0$ K to 13. Considering the polycrystalline average $(2 \cdot \theta_P^a + \theta_P^c)/3$ of both sets of values, the Kondo temperature of the substituted samples decreases moderately (from 12 K to 9 K) which is in conflict with the T_K evolution derived from the specific heat. According to a general rule [22], the $4f$ -ligand hybridization weakens with increasing cell volume. Taking into account the probable weakening of the hybridization strength when Pd is substituted instead of Rh, one might expect naively that T_K decreases with increasing Pd concentration instead of its enhancement as proposed by the two-level model above; thus the model seems to be inappropriate in the case of the $\text{Ce}_2\text{Rh}_{1-x}\text{Pd}_x\text{In}_8$ series. The increasing cell volume would also suggest an increase of the robustness of the AF order. However, T_N decreases with the Pd content which points to a combined effect of more energy scales playing important role in the series including the exchange interaction.

Table 1

Concentration dependence of the paramagnetic Curie temperature θ_P and the effective magnetic moment μ_{eff} of $\text{Ce}_2\text{Rh}_{1-x}\text{Pd}_x\text{In}_8$ ($x = 0, 0.15, 0.85, 1$).

x	θ_P (K)		μ_{eff} (μ_B/Ce)	
	$\parallel a$	$\parallel c$	$\parallel a$	$\parallel c$
0	-68	-8	2.5	2.6
0.15	-60	-3	2.4	2.4
0.85	-48	-17	2.3	2.4
1	-90	-50	2.6	2.6

The concentration dependence of the magnetic-ordering temperature T_N and the electronic Sommerfeld coefficient are depicted in the temperature-concentration diagram in Fig. 5. For T_{LN} for Ce_2RhIn_8 and T_c for Ce_2PdIn_8 , only one single point is shown because no signs of these transitions have been found for the neighboring compositions $\text{Ce}_2\text{Rh}_{0.9}\text{Pd}_{0.1}\text{In}_8$ and $\text{Ce}_2\text{Rh}_{0.15}\text{Pd}_{0.85}\text{In}_8$. Apparently, no overlap of superconductivity and antiferromagnetism is observed at temperatures above 0.35 K, i.e. either the phenomena do not coexist and they are well separated in a specific concentration range or the coexistence is hidden at temperatures below 0.35 K.

The critical concentration where T_N goes to zero can be extrapolated to $x \sim 0.45$. The low-temperature upturn of the C/T curve observed in this concentration region suggests presence of quantum fluctuations [20]. As the C/T upturn reduces before x approaches 1, the quantum fluctuations are likely not related to the superconductivity of Ce_2PdIn_8 .

Similar to the Co [10] and Ir [7] substitutions, Pd substitution in Ce_2RhIn_8 suppresses gradually the AF order. Nevertheless, the magnetism of $\text{Ce}_2\text{Rh}_{1-x}\text{Pd}_x\text{In}_8$ is more sensitive to the Pd concentration than to the isoelectronic substitutions ($T = \text{Co}, \text{Ir}$) because T_N is suppressed rapidly at low Pd content. The $\text{Ce}_2\text{Rh}_{1-x}\text{Co}_x\text{In}_8$ and $\text{Ce}_2\text{Rh}_{1-x}\text{Pd}_x\text{In}_8$ systems do not reveal any SC transition for magnetically ordered samples. As Ce_2CoIn_8 ($T_c = 0.4$ K [26]) and Ce_2PdIn_8 are HF superconductors, one might recognize similarities of the corresponding T - x phase diagrams. According to Ref. 7, the occurrence of the SC phases becomes unfavorable for alloys with $n = 2$ due to the higher dimensionality and stronger disorder. This scenario is supported by the fact that the SC state is suppressed in Ce_2PdIn_8 immediately after introducing Rh substitution. Unfortunately, the phase diagram of $\text{Ce}_2\text{Rh}_{1-x}\text{Co}_x\text{In}_8$ is not known for $0.6 < x < 1$ which prevents us from any further speculations.

Comparison of $\text{Ce}_2\text{Rh}_{1-x}\text{Pd}_x\text{In}_8$ and the related $\text{CeRh}_{1-x}\text{Pd}_x\text{In}_5$ alloys [19] shows that the suppression of magnetic order by moderate concentrations of Pd ($x < 0.3$) is stronger in the systems with $n = 2$. Similar behavior is observed for compounds substituted with Co and Ir compared to their more 2D counterparts ($n = 1$) [9,27].

The character of the phase diagram (Fig. 5) resembles recently published results for the tetragonal $\text{CeRh}(\text{In},\text{Sn})_5$ [28] and $\text{U}_2\text{Pt}_x\text{Rh}_{1-x}\text{C}_2$ [20] systems. In the Sn-substituted CeRhIn_5 , the magnetic order is suppressed at a critical concentration $x_c \sim 0.35$ and no superconductivity appears around this concentration. In $\text{U}_2\text{Pt}_x\text{Rh}_{1-x}\text{C}_2$, the antiferromagnetism is suppressed completely at $x \sim 0.7$ whereas the superconductivity emerges above $x \sim 0.9$; thus, no coexistence of both phenomena is present in these systems. Similar to the present results, a low-temperature upturn of the specific heat is observed for the critical concentrations; in the case of $\text{Ce}_2\text{Rh}_{1-x}\text{Pd}_x\text{In}_8$, it is accompanied with a simultaneous increase of the γ coefficient.

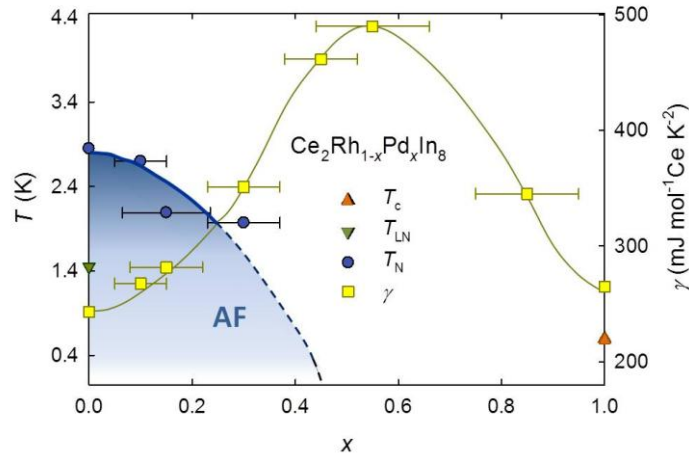


Fig. 5. T - x phase diagram of $\text{Ce}_2\text{Rh}_{1-x}\text{Pd}_x\text{In}_8$ based on the results of specific-heat measurements. The temperatures T_N , T_{LN} and T_c are presented by the left axis; the Sommerfeld coefficient γ by the right axis. The solid lines are guides to the eyes; the dashed line is an extrapolation of the data to the zero value of T_N : the critical concentration is $x \sim 0.45$. The error bars have been obtained from the microprobe analysis.

4. Conclusions

$\text{Ce}_2\text{Rh}_{1-x}\text{Pd}_x\text{In}_8$ ($x = 0, 0.1, 0.15, 0.3, 0.45, 0.55, 0.85, 1$) single crystals have been successfully grown by means of the In self-flux method. A series of specific-heat and magnetization measurements has been performed in order to study the effect of Pd substitution on the ground-state properties of Ce_2RhIn_8 . The measurements show that the Néel temperature T_N is gradually suppressed upon Pd substitution and, simultaneously, the Sommerfeld coefficient γ is enhanced. The AF order vanishes at a critical concentration $x \sim 0.45$; the maximum of the $\gamma(x)$ curve corresponds to this critical concentration region where no magnetic order is observed and, moreover, the emergence of critical fluctuations reflected in the low-temperature specific-heat upturn below $T = 1$ K coincides with this region. The order-to-order transition at T_{LN} and the magnetic field-induced transition T_m are also affected by the introduction of: increasing the Pd concentration suppresses T_{LN} immediately and T_m is not observable for Pd contents higher than $x > 0.15$. Ambient pressure superconductivity is not observed in any of the Rh-containing samples.

In general, the $\text{Ce}_2\text{Rh}_{1-x}\text{Pd}_x\text{In}_8$ single crystals have been found more sensitive to Pd substitution compared to the isoelectronic substitutions with Co and Ir [7,10] and also compared to their 2D $\text{CeRh}_{1-x}\text{Pd}_x\text{In}_5$ analogs [19]. The T - x phase diagram suggests that magnetic order and superconductivity do not coexist in this system and shows that both phenomena are well separated in the concentration range $0.3 < x < 1$. Nevertheless, the slight possibility that coexistence of magnetic order and superconductivity may be hidden at temperatures which are not accessible with our experimental equipment cannot be entirely excluded. Further low-temperature studies are desired to resolve this still open question.

Acknowledgements

This work was supported by the Grant Agency of Charles University (Project no. 134214) and by the Czech Science Foundation (Project no. GP14-17102P). Experiments were performed at MLTL (<http://mltl.eu/>), which is supported within the program of Czech Research Infrastructures (Project no. LM2011025).

References

- [1] C. Pfleiderer, Rev. Mod. Phys. 81 (2009) 1551.
- [2] J. D. Thompson, R. Movshovich, Z. Fisk, F. Bouquet, N. J. Curro, R. A. Fisher, P. C. Hammel, H. Hegger, M. F. Hundley, M. Jaime, P. G. Pagliuso, C. Petrovic, N. E. Phillips, J. L. Sarrao, J. Magn. Mater. 226-230 (2001) 5.
- [3] M. Kratochvilova, M. Dusek, K. Uhlirova, A. Rudajevova, J. Prokleska, B. Vondrackova, J. Custers, V. Sechovsky, J. Cryst. Growth 397 (2014) 47.
- [4] A. Malinowski, M. F. Hundley, N. O. Moreno, P. G. Pagliuso, J. L. Sarrao, J. D. Thompson, Phys. Rev. B 68 (2003) 184419.
- [5] W. Bao, P. G. Pagliuso, J. L. Sarrao, J. D. Thompson, Z. Fisk, J. W. Lynn, Phys. Rev. B 64 (2001) 020401.
- [6] M. Nicklas, V. A. Sidorov, H. A. Borges, P. G. Pagliuso, C. Petrovic, Z. Fisk, J. L. Sarrao, J. D. Thompson, Phys. Rev. B 67 (2003) 020506.
- [7] E. N. Hering, H. A. Borges, S. M. Ramos, M. B. Fontes, E. Baggio-Saitovich, M. A. Continentino, E. M. Bittar, L. M. Ferreira, R. Lora-Serrano, F. C. G. Gandra, C. Adriano, P. G. Pagliuso, N. O. Moreno, J. L. Sarrao, J. D. Thompson, Phys. Rev. B 82 (2010) 184517.
- [8] C. Adriano, C. Giles, E. M. Bittar, L. N. Coelho, F. de Bergevin, C. Mazzoli, L. Paolasini, W. Ratcliff, R. Bindel, J. W. Lynn, Z. Fisk, P. G. Pagliuso, Phys. Rev. B 81 (2010) 245115.
- [9] M. Nicklas, V. A. Sidorov, H. A. Borges, P. G. Pagliuso, J. L. Sarrao, J. D. Thompson, Phys. Rev. B 70 (2004) 020505.
- [10] N. O. Moreno, M. F. Hundley, P. G. Pagliuso, R. Movshovich, M. Nicklas, J. D. Thompson, J. L. Sarrao, Z. Fisk, Physica B 312 (2002) 274.
- [11] arXiv:1502.02544
- [12] K. Ohishi, T. Suzuki, R. H. Heffner, T. U. Ito, W. Higemoto, E. D. Bauer, J. Phys.: Conference Series 225 (2010) 012042.
- [13] P. G. Pagliuso, N. O. Moreno, N. J. Curro, J. D. Thompson, M. F. Hundley, J. L. Sarrao, Z. Fisk, A. D. Christianson, A. H. Lacerda, B. E. Light, A. L. Cornelius, Phys.

- Rev. B 66 (2002) 054433.
- [14] S. Ohara, K. Ohno, T. Miyake, K. Tsuji, T. Yamashita, I. Sakamoto, *Physica C* 470 (2010) 573.
 - [15] K. Uhlirova, J. Prokleska, V. Sechovsky, S. Danis, *Intermetallics* 18 (2010) 2025.
 - [16] K. Uhlirova, J. Prokleska, V. Sechovsky, *Phys. Rev. Lett.* 104 (2010) 059701.
 - [17] D. Kaczorowski, A. P. Pikul, D. Gnida, V. H. Tran, *Phys. Rev. Lett.* 104 (2010) 059702.
 - [18] J. K. Dong, H. Zhang, X. Qiu, B. Y. Pan, Y. F. Dai, T. Y. Guan, S. Y. Zhou, D. Gnida, D. Kaczorowski, S. Y. Li, *Phys. Rev. X* 1 (2011) 011010.
 - [19] M. Kratochvilova, K. Uhlirova, J. Prchal, J. Prokleska, M. Misek, V. Sechovsky, *J. Phys.: Condens. Matter*, 27 (2015) 095602.
 - [20] N. Wakeham, N. Ni, E. D. Bauer, J. D. Thompson, E. Tegtmeier, F. Ronning, *Phys. Rev. B* 91 (2015) 024408.
 - [21] T. Ueda, H. Shishido, S. Hashimoto, T. Okubo, M. Yamada, Y. Inada, R. Settai, H. Harima, A. Galatanu, E. Yamamoto, N. Nakamura, K. Sugiyama, T. Takeuchi, K. Kindo, T. Namiki, Y. Aoki, H. Sato, Y. Ōnuki, *J. Phys. Soc. Jpn.* 73 (2004) 649.
 - [22] J. A. Blanco, M. Depodesta, J. I. Espeso, J. C. G. Sal, C. Lester, K. A. Mcewen, N. Patrikios, and J. R. Fernandez, *Phys. Rev. B* 49 (1994) 15126.
 - [23] A. L. Cornelius, P. G. Pagliuso, M. F. Hundley, J. L. Sarrao, *Phys. Rev. B* 64 (2001) 144411.
 - [24] H. Hegger, C. Petrovic, E. G. Moshopoulou, M. F. Hundley, J. L. Sarrao, Z. Fisk, and J. D. Thompson, *Phys. Rev. Lett.* 84 (2000) 4986.
 - [25] A. C. Hewson, *The Kondo Problem to Heavy Fermions* (1997) Cambridge University Press, Cambridge.
 - [26] G. F. Chen, S. Ohara, M. Hedo, Y. Uwatoko, K. Saito, M. Sorai, and I. Sakamoto, *J. Phys. Soc. Jpn.* 71 (2002) 2836.
 - [27] P. G. Pagliuso, R. Movshovich, A. D. Bianchi, M. Nicklas, N. O. Moreno, J. D. Thompson, M. F. Hundley, J. L. Sarrao, Z. Fisk, *Physica B* 312 (2002) 129.
 - [28] S. Raymond, J. Buhot, E. Ressouche, F. Bourdarot, G. Knebel, G. Lapertot, *Phys. Rev. B* 90 (2014) 014423.